Lasers in Manufacturing Conference 2017

Time-resolved temperature measurement during laser marking of stainless steel

Martin Kučera[a, *], Jiří Martan[a]

[a] *New Technologies Research Centre (NTC), University of West Bohemia, Univerzitni 8, 306 14 Pilsen, Czech Republic*

Abstract

Laser marking is a well-established technology in industry; however there are still issues where the marking process itself needs to be investigated. The surface microstructure and the phase composition can be changed by the laser treatment. For this reason we present a study of temperatures reached by different parameters of laser marking and their correlation with resulted microstructure and phase composition. The marking was done using nanosecond pulsed fibre laser with variable pulse duration (from 9 to 200 ns), repetition frequency and pulse energy. Similar marking was obtained by different parameters but different phase composition and it correlates well with maximum temperatures reached in the laser spot, which varied from less than 1100°C to more than 1800°C. From the results it can be concluded that combination of longer pulse duration and higher repetition rate are the most suitable parameters for achieving the stainless steel marking without surface melting.

Keywords: time resolved temperature measurement; laser; marking; stainless steel

1. Motivation

The knowledge of temperatures of the material surface during the laser irradiation is important for understanding of the processes during laser processing of material. For the temperature field measurement during the pulsed laser heating of the surface of the material there are used different experimental methods based on different physical principles. Frequently there are used procedures which combine several methods together to compare and verify the results. For example for the investigation of the dynamics of melting and

* Corresponding author.
E-mail address: kucera82@ntc.zcu.cz .

resolidification of the a-Si thin film Moon, Lee, & Grigoropoulos, 2002, the reflectivity, transmissivity, emission and electrical conductance are measured.

1.1. The methods for surface temperature measurement

The methods for surface temperature measurement can be classified according to following criteria: the principle of the method, the used detector, the response time, the temperature range and the output of the method. There are used methods based on the electrical conductance measurement Grigoropoulos & Bennett, 1996, on the reflectivity or transmissivity of the measuring laser D.H. Lowndes, G.E. Jellison, R.F. Wood, 1984, on the VIS, NIR and IR radiation measurement of the sample surface Ignatiev & Smurov, 1996, Doubenskaia & Smurov, 2006 Doubenskaia, Bertrand, & Smurov, 2006, the detection of the Raman scattering induced by the measuring laser Hashimoto, 2015 or XRD diffraction Buschert et al., 1989. The most often is used the time-resolved reflectivity measurement than the emission measurement using pyrometry or other radiometric methods. To achieve the time resolution in the microseconds and space resolution in the micrometers the contact methods are failing and also the standard pyrometers and IR techniques doesn't work due to lack of the space resolution or unknown emissivity value Kappes, Li, Butt, & Gutmann, 2010.

2. The experimental systems

- The samples

The investigated material was a cold-rolled AISI 304 stainless steel. Experimental samples were 1.5 mm thick sheets with the surface quality 2R (polished). The microstructure of the steel is austenitic with marks of plastic deformation.

- Laser marking system

Pulsed fibre laser SPI G3-HS of 20 W maximum average output power with SCANLAB SCANcube 10 scanning head with 160 mm f-theta lens was used for laser marking experiments. The laser spot diameter 1/e2 was 65 micrometres.

- Temperature measurement system

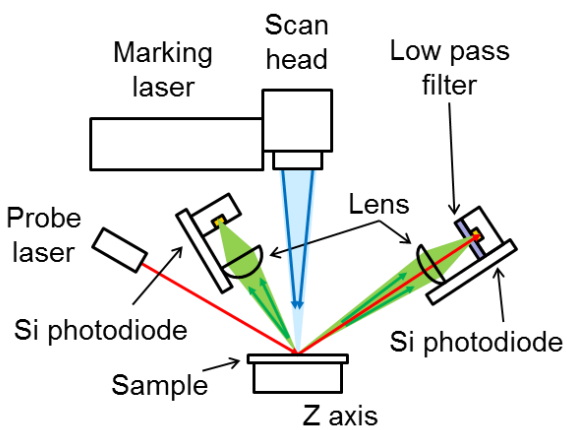

Fig. 1. Schematic representation of the experimental system.

The sample irradiated (heated) by a pulsed fibre laser at 1064 nm emits infrared radiations from its surface. The emitted radiation is focused by a lens, focal length 50 mm, and transmitted through the shortpass filter *Thorlabs FES1000*, which eliminates the reflected laser radiation at 1064 nm. The filter *FES1000* transmissivity for wavelengths from 700 to 1000 nm is higher than 90 % and the optical density for laser wavelength 1064 nm is higher than 5. The radiation is focused by the lens to the silicon PIN photodiode *Hamamatsu S5052*. The PIN photodiode operates with a reverse voltage applied and the response speed is 500 MHz. The spectral sensitivity is in the range from 300 to 1100 nm.

Simultaneously with the emitted radiation measurement, the phase and structural changes are detected by the time-resolved reflectivity (TRR) method described in Semmar, Tebib, Tesar, Puscas, & Amin-Chalhoub, 2009. The He-Ne cw laser is directed onto heated zone of the sample. The reflected light is focused by the lens, focal length 25.4 mm, onto the silicon PIN photodiode Hamamatsu S5972. The reflectivity of the probe laser depends on the temperature and the phase variations of the sample's surface. The obtained signals are then recorded on a digital oscilloscope (500 MHz).

3. Calibration

In order to obtain the absolute surface temperature, the PIN photodiode output was calibrated. The spectral sensitivity of the detector (PIN diode S5052) with the filter FES1000 is obtained by multiplication of the sensitivity of the diode S5052 and transmissivity of the filter FES1000 for the wavelengths in range from 300 to 1100 nm. The voltage sensitivity of the detector $y_V(\lambda)$ [V/W] was obtained by interpolating of the spectral sensitivity of the detector S5052 with the filter FES1000 with the step 1 nm in the range from 300 to 1100 nm and multiplication with the gain of the detector system.

The theoretical calibration curve $U_0(T)$ was obtained by numerical integration across wavelengths of the spectral power density given by the Planck's law, multiplied by the voltage sensitivity of the detector $y_V(\lambda)$ and the detector sensitive area S. The integration was done for temperatures in the range from 300 to 10 000 K.

$$U_0(T) = S \int y_V(\lambda) \frac{2\pi c^2 h \lambda^{-5}}{exp\left(\frac{ch}{\lambda kT}\right) - 1} d\lambda \qquad (1)$$

To obtain the dependence $U_1(T)$, which includes the geometrical configuration, optical configuration and the emissivity, the multiplication constant k was used. This constant k was determined from the measurement where the absolute surface temperature of the sample was known (phase transition temperature of the material).

$$U_1(T) = k \cdot U_0(T) \qquad (2)$$

The function $T(U_1)$ for the calculation of the absolute surface temperature from the measured voltage was obtained by numerical inversion of the function $U_1(T)$.

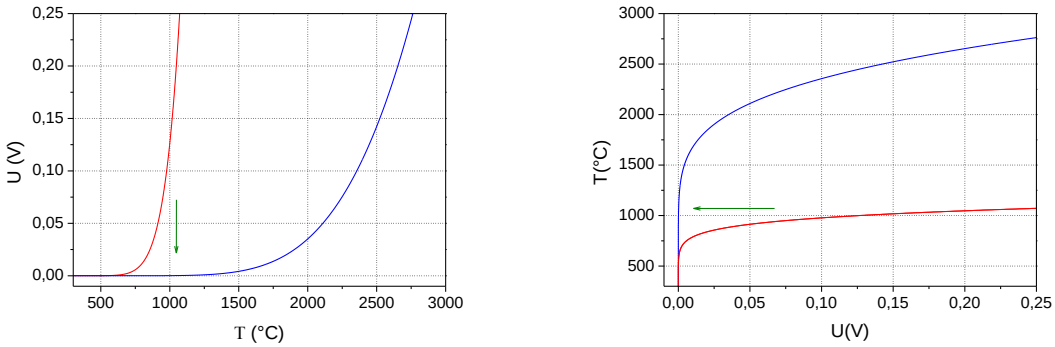

Fig. 2. The theoretical calibration curve (red) and fitted dependence by multiplication constant (blue), the resulting function for the absolute temperature determination (right).

For the multiplication factor determination, measurements with the melting and solidification were performed. The solidification phase change was observed at the TRR and IR emission signals. The delay on constant temperature is present in time from 2300 to 2700 ns is in the measured voltage on the IR emission detector and the TRR signal, which are displayed on the Fig. 3. The match of these two measurements confirms that the phase transition – solidification occurs. The calibration was performed on the base of the known solidification temperature of the material (1700 K). The resulted dependence is $U_1(T) = 0.0021 \cdot U_0(T)$. On the Fig. 4 there is the measured time dependence of the temperature for the pulse length 200 ns and pulse energy 0.30 mJ. The delay caused by the solidification occurred in the time 600 to 750 ns after the beginning of the pulse.

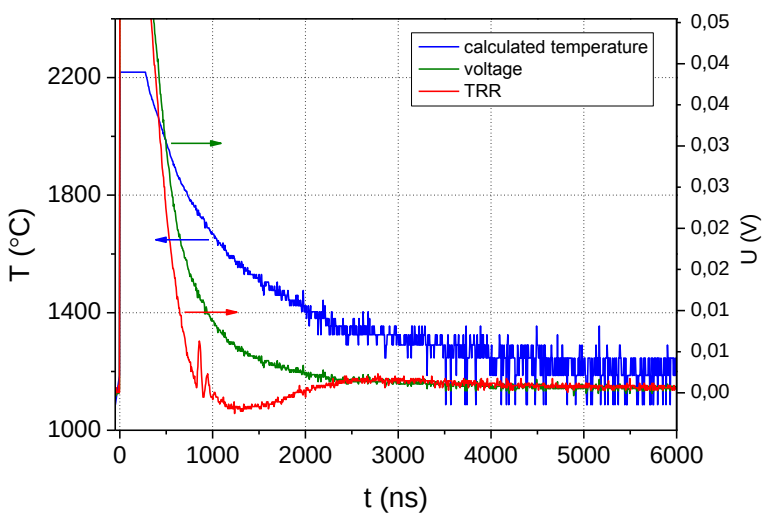

Fig. 3. The measured time dependencies of the voltage of the detectors IR emission and TRR signals with the calculated temperature based to the calibration curve. The pulse length is 200 ns, pulse energy 0.68 mJ and Ppd = 102.8 MW·cm^{-2}, frequency 25 kHz and scanning speed 800 mm·s^{-1}.

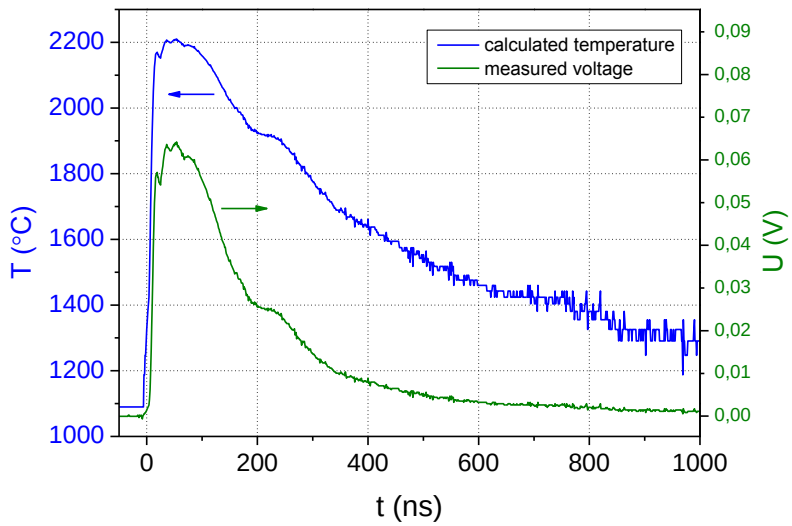

Fig. 4. The measured time dependencies for the pulse length 200 ns and pulse energy 0.30 mJ: the IR emission (voltage) and the temperature calculated based on the calibration curve.

4. Results

With the developed method, it was measured the time dependence of the surface temperature for the various laser settings to obtain the dependencies of the temperature on the selected laser parameters.

4.1. The influence of the pulse energy

For the constant pulse length, the measured surface temperature rises with the rising pulse energy, Fig. 5. The whole time dependence of the temperature **Fehler! Verweisquelle konnte nicht gefunden werden.**shifts with the rising pulse energy toward to the higher temperatures and the length of the solidification phase extends.

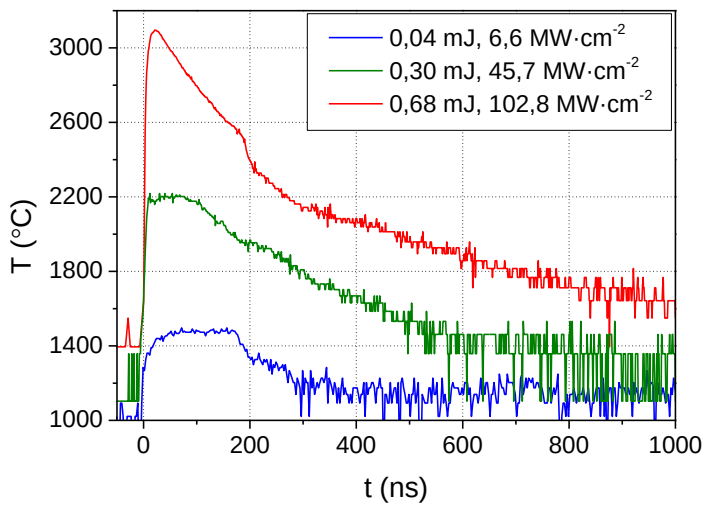

Fig. 5. The measured temperature dependence for the pulse length 200 ns, various pulse energies, frequency 25 kHz and scanning speed 800 mm·s^{-1}.

4.2. The influence of the pulse length and the pulse energy

For the longer pulse length 160 ns and pulse energy 0.09 mJ, Fig. 6, the measured surface temperatures reach 1200°C (frequency 200 kHz). These measured temperatures are under the melting temperature of the AISI 304 steel which is 1427°C Adams et al., 2013. For the lower pulse energies 0.04 mJ and frequency 400 kHz the surface temperature cannot be measured, because it was under the detection limit 1100 °C.

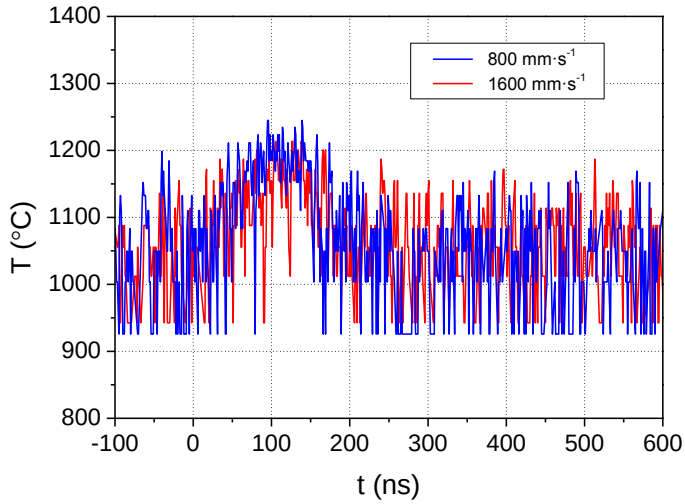

Fig. 6. The measured temperature dependence for the pulse length 160 ns, various scanning speeds, frequency 200 kHz, pulse energy 0.09 mJ a P_{pd} = 13.1 MW·cm^{-2}.

The measured surface temperatures for the short pulse length 15 ns and pulse energy 0.07 mJ are shown in Fig. 7. The maximum temperature exceeds 1800°C, which is well above the melting temperature.

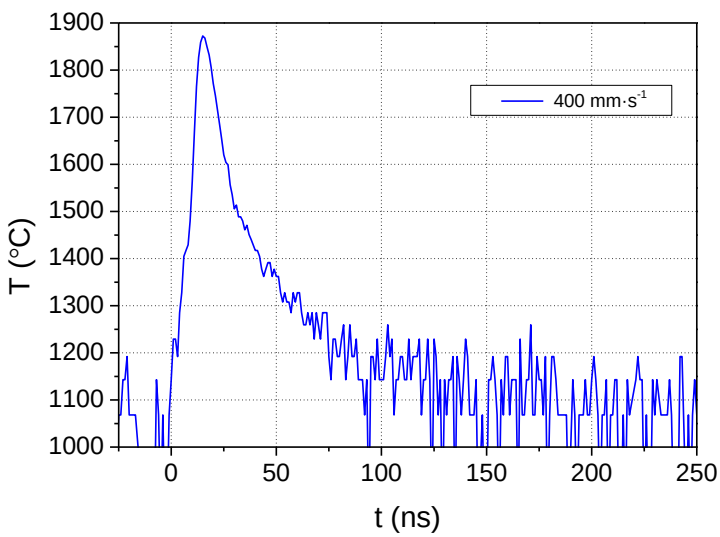

Fig. 7. The measured temperature dependence for the pulse length 15 ns, scanning speed 400 mm·s^{-1}, frequency 250 kHz, pulse energy 0.07 mJ a P_{pd} = 138 MW·cm^{-2}.

5. Conclusion

New measurement system was developed for time resolved temperature measurement during pulsed laser processing of material. It was used to study surface temperatures during laser marking of stainless steel by a nanosecond laser. The system and its calibration were described. The multiplication calibration coefficient was determined based on solidification time delay during cooling phase after the laser pulse. For high energy densities temperatures above 3000°C were observed during tests with laser pulses. For the marking process the measured temperatures ranged from less than 1100°C for longer pulses to more than 1800°C for shorter pulses. The shorter pulses (15 ns) induce surface temperature much higher than melting temperature of the stainless steel and can have significant effects on the material microstructure on surface and on its corrosion resistance during the use of the marked part. So for marking process, where the melting of the surface is not suitable, longer pulse durations than 150 ns should be used.

Acknowledgements

The work has been supported by the Ministry of Education, Youth and Sports of the Czech Republic (OP RDI program, CENTEM project, no. CZ.1.05/2.1.00/03.0088, co-funded by the ERDF; NPU I program, CENTEM PLUS project no. LO1402) and project SGS-2016-005.

References

Adams, D. P., Hodges, V. C., Hirschfeld, D. A., Rodriguez, M. A., McDonald, J. P., & Kotula, P. G. (2013). Nanosecond pulsed laser irradiation of stainless steel 304L: Oxide growth and effects on underlying metal. *Surface and Coatings Technology*, *222*, 1–8. https://doi.org/10.1016/j.surfcoat.2012.12.044

Buschert, J. R., Tischler, J. Z., Mills, D. M., Colella, R., Lafayette, W., & Introduction, I. (1989). Time resolved x-ray diffraction study of laser annealing in silicon at grazing incidence. *Journal of Applied Physics*, *66*(October 1989), 3523–3525.

D.H. Lowndes, G.E. Jellison, R.F. Wood, R. C. (1984). Time-resolved studies of ultrarapid solidification of highly undercooled molten silicon formed by pulsed laser. *27 Th INTERNATIONAL CONFERENCE ON THE PHYSICS OF SEMICONDUCTORS*.

Doubenskaia, M., Bertrand, P., & Smurov, I. (2006). Pyrometry in laser surface treatment. *Surface and Coatings Technology*, *201*(5), 1955–1961. https://doi.org/10.1016/j.surfcoat.2006.04.060

Doubenskaia, M., & Smurov, I. (2006). Surface temperature evolution in pulsed laser action of millisecond range. *Applied Surface Science*, *252*(13 SPEC. ISS.), 4472–4476. https://doi.org/10.1016/j.apsusc.2005.07.164

Grigoropoulos, C. P., & Bennett, T. E. D. D. (1996). *Heat and Mass Transfer Phase Transformations* (Vol. 28).

Hashimoto, F. (2015). Time-resolved Micro-Raman Measurement of Temperature Dynamics during High-Repetition-Rate Ultrafast Laser Microprocessing. *Journal of Laser Micro/Nanoengineering*, *10*(1), 29–32. https://doi.org/10.2961/jlmn.2015.01.0006

Ignatiev, M. B., & Smurov, I. Y. (1996). Surface temperature measurements during pulsed laser action on metallic and ceramic materials. *Applied Surface Science*, *96–98*, 505–512. https://doi.org/10.1016/0169-4332(95)00504-8

Kappes, R. S., Li, C., Butt, H.-J., & Gutmann, J. S. (2010). Time-resolved, local temperature measurements during pulsed laser heating. *New Journal of Physics*, *12*(8), 83011. https://doi.org/10.1088/1367-2630/12/8/083011

Moon, S.-J., Lee, M., & Grigoropoulos, C. P. (2002). Heat Transfer and Phase Transformations in Laser Annealing of Thin Si Films. *Journal of Heat Transfer*, *124*(2), 253. https://doi.org/10.1115/1.1447941

Semmar, N., Tebib, M., Tesar, J., Puscas, N. N., & Amin-Chalhoub, E. (2009). Direct observation of phase transitions by time-resolved pyro/reflectometry of KrF laser-irradiated metal oxides and metals. *Applied Surface Science*, *255*(10), 5549–5552. https://doi.org/10.1016/j.apsusc.2008.08.084